Research

Natural variation in *Avr3D1* from *Zymoseptoria* sp. contributes to quantitative gene-for-gene resistance and to host specificity

Lukas Meile[1,2] (iD), María Garrido-Arandia[1,2,3]* (iD), Zoe Bernasconi[1]* (iD), Jules Peter[1]*, Alissa Schneller[1], Alessio Bernasconi[1] (iD), Julien Alassimone[1], Bruce A. McDonald[1] (iD) and Andrea Sánchez-Vallet[1,2] (iD)

[1]Plant Pathology, Institute of Integrative Biology, ETH Zurich, Universitätstrasse 2, Zurich 8092, Switzerland; [2]Centro de Biotecnología y Genómica de Plantas, Universidad Politécnica de Madrid (UPM)–Instituto Nacional de Investigación y Tecnología Agraria y Alimentaria (INIA), 28223 Pozuelo de Alarcón, Madrid, Spain; [3]Departamento de Biotecnología-Biología Vegetal, Escuela Técnica Superior de Ingeniería Agronómica, Alimentaria y de Biosistemas, Universidad Politécnica de Madrid (UPM), 28040 Madrid, Spain

Summary

- Successful host colonization by plant pathogens requires the circumvention of host defense responses, frequently through sequence modifications in secreted pathogen proteins known as avirulence factors (Avrs). Although Avr sequences are often polymorphic, the contribution of these polymorphisms to virulence diversity in natural pathogen populations remains largely unexplored.
- We used molecular genetic tools to determine how natural sequence polymorphisms of the avirulence factor Avr3D1 in the wheat pathogen *Zymoseptoria tritici* contributed to adaptive changes in virulence.
- We showed that there is a continuous distribution in the magnitude of resistance triggered by different Avr3D1 isoforms and demonstrated that natural variation in an *Avr* gene can lead to a quantitative resistance phenotype. We further showed that homologues of Avr3D1 in two nonpathogenic sister species of *Z. tritici* are recognized by some wheat cultivars, suggesting that Avr-R gene-for-gene interactions can contribute to nonhost resistance.
- We suggest that the mechanisms underlying host range, qualitative resistance, and quantitative resistance are not exclusive.

Introduction

The success of a pathogen is determined largely by its capacity to overcome or avoid host immune responses (Schulze-Lefert & Panstruga, 2011; Ayliffe & Sørensen, 2019; Panstruga & Moscou, 2020). Plants and pathogens are engaged in a molecular arms-race, characterized by the co-evolution of a multilayered host immune system and of diverse pathogen adaptation strategies to prevent the induction of immune responses (Jones & Dangl, 2006; Cook *et al.*, 2015; Toruño *et al.*, 2016). The ability to overcome plant immunity depends mainly on pathogen effector proteins, which enable host colonization by interfering with plant defenses, signaling, and development (Hogenhout *et al.*, 2009; Lo Presti *et al.*, 2015; Toruño *et al.*, 2016). Although effectors generally provide an advantage to the pathogen, they can be recognized by resistance (R) proteins present in certain host genotypes, triggering a defense response (Flor, 1971; Stergiopoulos & de Wit, 2009). The recognized effectors therefore restrict pathogen virulence and in these cases are known as avirulence factors (Avrs). Consequently, there is a strong evolutionary pressure acting on *Avr* genes to escape recognition while maintaining their effector function (Bent & Mackey, 2007).

Quantitative resistance, which describes any kind of resistance which is not complete, is frequently considered polygenic, broad-spectrum, and diverse in mechanisms (Cowger & Brown, 2019; Karasov *et al.*, 2020). By contrast, the determination of the disease outcome by pairs of pathogen *Avr* and plant *R* genes is a simple two-component genetic interaction, which has been described as the gene-for-gene model of plant–pathogen compatibility (Flor, 1971). This Avr-R protein interaction frequently leads to the induction of a strong immune response that fully arrests disease progression in an isolate-specific manner (Sánchez-Martín & Keller, 2021). Therefore, gene-for-gene resistance is commonly considered a qualitative trait that will lead to either a compatible or an incompatible interaction. It is frequently assumed that this type of interaction does not lead to intermediate phenotypes (Karasov *et al.*, 2020; Sánchez-Martín & Keller, 2021). Pathogens that harbor *Avr* genes can evolve to escape Avr recognition through modifications of the *Avr* coding sequence (Fudal *et al.*, 2009; Kanzaki *et al.*, 2012; Zhong *et al.*, 2017; Meile *et al.*, 2018), but also through other mechanisms, including *Avr* gene deletions (Rouxel *et al.*, 2003; Gilroy *et al.*, 2011; De Jonge *et al.*, 2012; Hartmann *et al.*, 2017) and changes in *Avr* gene

---

*These authors contributed equally to this work.

expression (Qutob *et al.*, 2013; Wu *et al.*, 2015). As a result of pathogen evolution toward host evasion, fungal avirulence genes are frequently highly polymorphic in pathogen populations and under diversifying selection. Mutations in *Avr* sequences have been frequently linked to host evasion in the context of classic gene-for-gene interactions featuring major *R* genes and large effects on the disease outcome. However, although quantitative resistance and gene-for-gene interactions are not conceptually exclusive, small phenotypic effects of *Avr* gene mutations have been investigated in only a few pathosystems, including leaf rust, flax rust, and rice blast (Zenbayashi-Sawata *et al.*, 2005; Wang *et al.*, 2007; Marcel *et al.*, 2008; Poland *et al.*, 2009; Maqbool *et al.*, 2015; Niks *et al.*, 2015; Zhang *et al.*, 2018; Cowger & Brown, 2019). This is despite the possibility that many small phenotypic contributions of different Avr mutations could substantially shape the overall fitness of pathogens, with consequences on virulence evolution and, hence, the development of strategies to increase the durability of resistance in crops (Cowger & Brown, 2019).

Although Avr recognition has traditionally been investigated in the context of resistance against host-adapted pathogens, increasing evidence indicates that Avr recognition is also involved in nonhost resistance (Schulze-Lefert & Panstruga, 2011; Bettgenhaeuser *et al.*, 2018; Gilbert *et al.*, 2018; Ayliffe & Sørensen, 2019). For example, the capacity of cereal mildews to infect wheat was shown to be controlled by recognition of AvrPm3 (Bourras *et al.*, 2019) and the emergence of wheat blast was shown to be facilitated by the widespread use of wheat cultivars lacking the *Rwt3* resistance gene (Inoue *et al.*, 2017). Thus, the repertoire of effectors present in a pathogen largely defines its compatibility with a host genotype or even a host species (Ayliffe & Sørensen, 2019), not only because effector function can be highly specialized toward certain hosts (Walton, 1996; Dong *et al.*, 2014), but also because of effector recognition by resistance proteins (Sánchez-Vallet *et al.*, 2018; Frantzeskakis *et al.*, 2019).

Zymoseptoria tritici is a highly specialized wheat pathogen that originated 10 000–11 000 yr ago during wheat domestication (Stukenbrock *et al.*, 2007). The closely related *Zymoseptoria* species *Z. pseudotritici* and *Z. ardabiliae* are pathogenic on wild grasses, but not on wheat (Stukenbrock *et al.*, 2012). The genomes of these three *Zymoseptoria* species are highly similar, with 6% divergence at the nucleotide level between *Z. tritici* and *Z. pseudotritici* and 10% between *Z. tritici* and *Z. ardabiliae* (Stukenbrock *et al.*, 2011). Consequently, several effector genes of *Z. tritici* are also found in the genomes of *Z. pseudotritici* and *Z. ardabiliae* (Stukenbrock *et al.*, 2011; Feurtey *et al.*, 2019). Although effectors have been suggested to be involved in adaptation of *Z. tritici* to wheat, their role in host specialization remains unclear (Stukenbrock *et al.*, 2011; Poppe *et al.*, 2015; Lorrain *et al.*, 2021). *Zymoseptoria tritici* is a fast-evolving pathogen with a mixed reproduction system and a large effective population size that has frequently overcome resistance genes deployed by wheat breeding (McDonald & Mundt, 2016). Despite efforts to characterize resistance to *Z. tritici*, the mechanisms of escape from recognition are not well-understood. The only two *Avr* genes that have been cloned, *Avr3D1* and *AvrStb6*, are present in all or

nearly all the strains investigated so far, are highly polymorphic and under diversifying selection (Zhong *et al.*, 2017; Brunner & McDonald, 2018; Meile *et al.*, 2018; Stephens *et al.*, 2021). The recognition of Avr3D1 by some wheat lines triggers a quantitative resistance (Meile *et al.*, 2018), whereas recognition of AvrStb6 leads to a qualitative resistance phenotype (Zhong *et al.*, 2017; Kema *et al.*, 2018). *Avr3D1* is ubiquitously present and highly diverse in *Z. tritici* populations. Thirty different protein isoforms of Avr3D1 were identified in 132 strains collected from four different global wheat populations (Meile *et al.*, 2018). However, the contribution of *Avr3D1* mutations in natural populations of *Z. tritici* to host adaptation remains unknown.

Here, we explore the natural diversity of *Avr3D1* with respect to the effect of various mutations on the disease outcome. We show that homologues of Avr3D1 from the sister species *Z. ardabiliae* and *Z. pseudotritici* are recognized in wheat, suggesting that Avrs can determine host range and nonhost resistance. Additionally, we demonstrate that differences in recognition of Avr3D1 isoforms by an R protein lead to differences in the penetration efficiency of the pathogen through the stomata and a continuous distribution in the magnitude of resistance (i.e. quantitative resistance) instead of two alternative phenotypes (resistant and susceptible). We also demonstrate that a large-effect quantitative trait locus can be partitioned into several moderate-effect amino acid substitutions that quantitatively contribute to host evasion. We conclude that quantitative gene-for-gene resistance phenotypes can result from a series of additive mutations in a single *Avr* gene.

Materials and Methods

Zymoseptoria tritici strains and genome resources

For the infection assays depicted below, we used a selection of previously described *Z. tritici* strains collected in four different countries (Switzerland (CH), Israel (ISY_Ar), USA (ORE) and Australia (AUS); Zhan *et al.*, 2005) as well as the Dutch reference strain IPO323 (Goodwin *et al.*, 2011). IPO323 harbors AvrStb6 and 3D1 harbors Avr3D1 (Zhong *et al.*, 2017; Kema *et al.*, 2018; Meile *et al.*, 2018). *Avr3D1* DNA and protein sequences were obtained from 132 strains (Zhan *et al.*, 2005; Torriani *et al.*, 2011; Plissonneau *et al.*, 2016, 2018; Hartmann *et al.*, 2017; Hartmann & Croll, 2017). To determine the *Avr3D1* sequence of strain IPO87019 (Kema *et al.*, 1996), filtered raw reads were downloaded from the JGI Genome Portal (Project ID: 1090932), assembled and subjected to BLAST search using the De Novo Assembly tool, the Extract Consensus Sequence tool and the BLAST tool implemented in CLC Genomics Workbench 9.5.4 (Qiagen, Aarhus, Denmark). The same software was used to identify a homologue of *Avr3D1* on chromosome 5 in strain 3D1. The *Avr3D1* sequences of strains ISR398 and ISR8036 (Yechilevich-Auster *et al.*, 1983) were determined by Sanger sequencing (Microsynth AG, Balgach, Switzerland) using amplicons generated with the Phusion polymerase (NEB, Ipswich, MA, USA) and primers depicted in Supporting Information Table S1 from genomic DNA in technical duplicates.

Identification of *Avr3D1* homologues in related *Zymoseptoria* species

We searched for homologues of *Avr3D1* using the BLAST tool implemented in CLC Genomics Workbench 11.0 in four strains of *Z. ardabiliae* (STIR04 1.1.1, STIR04 1.1.2, STIR04 3.13.1 and STIR04 3.3.2), five strains of *Z. pseudotritici* (STIR04 2.2.1, STIR04 3.11.1, STIR04 4.3.1, STIR04 5.3 and STIR04 5.9.1), one strain of *Zymoseptoria passerinii* (SP63), and one strain of *Zymoseptoria brevis* (Zb18110) using BLASTN (match cost: 2; mismatch cost: 3; gap existence cost: 5; gap extension cost: 2; word size: 11; filtered for low complexity). To determine the protein sequence of the homologues, their DNA sequences were aligned to the sequence of *Avr3D1*$_{3D1}$ using CLC Genomics Workbench 11.0 (Qiagen) to identify the start codon, the stop codon and intron 1 (Fig. S1). Signal peptide and effector predictions were performed using SignalP 3.0 (Dyrløv Bendtsen *et al.*, 2004) and EffectorP 1.0 (Sperschneider *et al.*, 2016), respectively. A maximum likelihood tree of protein sequences was obtained in CLC Genomics Workbench 11.0 (Qiagen) using the Jukes-Cantor distance and 100 bootstrap replications. The genome sequences were downloaded from NCBI (BioProject accession nos. PRJNA343332, PRJNA343333, PRJNA343334, PRJNA343335, PRJNA277173, PRJNA46489, PRJNA63035, PRJNA63037, PRJNA63039, PRJNA63049, and PRJNA273516 (Stukenbrock *et al.*, 2011; Grandaubert *et al.*, 2015)).

Generation of plasmid constructs and transformation of *Z. tritici* and *Z. ardabiliae*

To generate plasmid constructs for the ectopic expression of various alleles of *Avr3D1* in *Z. tritici*, we exchanged the coding DNA sequence (CDS) and intron 1 of *Avr3D1* in the plasmid pCGEN-*Avr3D1*$_{3D1}$ect, which had been generated in a previous study. In this plasmid, the *Avr3D1* promoter from the strain 3D1 is used to control the expression of *Avr3D1* (Meile *et al.*, 2018) under the name pCGEN-581$_{3D1}$ect. pCGEN-*Avr3D1*$_{3D1}$ect harbors the *Avr3D1* allele from strain 3D1 and is based on pCGEN, a plasmid designed for *Agrobacterium tumefaciens*-mediated transformation of fungi (Motteram *et al.*, 2011). To replace the CDS, pCGEN-*Avr3D1*$_{3D1}$ect was first digested with *Xho*I, removing the CDS and part of the promoter sequence. The resulting linearized plasmid, the amplified CDS of a different strain or species and a fragment to reconstitute the original promoter sequence were then assembled using the In-Fusion HD Cloning Kit (TaKaRa Bio Inc., Shiga, Japan), resulting in pCGEN-*Avr3D1*$_{strain\_of\_interest}$ect. The primers used for cloning are listed in Table S1 and the cloning procedure is illustrated in Fig. S2. GFP-expressing mutant lines were generated using the vectors pES1-Nat-GFP for *Z. tritici* strains and pCGEN-GFP for *Z. ardabiliae*. For pES1-Nat-GFP, we digested the vector pNAT-EctTF1(1A5) with the enzymes *Eco*RI and *Bcl*I, and for pCGEN-GFP, we digested the vector pCGEN with *Kpn*I. In both cases, we inserted the codon-optimized version of eGFP (Kilaru *et al.*, 2015). *Zymoseptoria tritici* and *Z. ardabiliae* were transformed by *A. tumefaciens*-mediated transformation

as described before (Zwiers & De Waard, 2001; Meile *et al.*, 2018), using the *A. tumefaciens* strain AGL-1. For the obtained mutants, the copy number of the inserted T-DNA was determined by qPCR on genomic DNA. Transformant lines with more than one T-DNA copy were excluded from further experiments.

Infection assays

Wheat seeds (*Triticum aestivum* L.) of cultivars Runal, Titlis and Drifter were purchased from DSP Ltd (Delley, Switzerland). Seeds of the wheat line ST6 (cultivar Estanzuela Federal) and the breeding line TE-9111 were gifts from Thierry Marcel and Marc-Henri Lebrun. ST6 harbors Stb7 and TE-9111 harbors Stb6, Stb7, and Stb11 (Brown *et al.*, 2015). Cultivar Runal recognizes Avr3D1 and therefore is considered to harbor Stb7. Titlis and Drifter do not recognize Avr3D1 (Meile *et al.*, 2018). Seedlings were grown before infection as previously described (Meile *et al.*, 2018). Briefly, the peat substrate Jiffy GO PP7 (Jiffy Products International, Moerdijk, the Netherlands) and square pots (11 × 11 × 12 cm) were used to grow seedlings for 15–18 d in a glasshouse at 18°C (day) and 15°C (night) with a 16-h photoperiod and 75% humidity.

To prepare *Z. tritici* inoculum, a dense blastospore suspension grown in yeast sucrose broth (YSB; 10 g l^{-1} yeast extract, 10 g l^{-1} sucrose, 50 μg ml^{-1} kanamycin sulfate) for 4–6 d (18°C, 120 rpm) was filtered through cheesecloth. Blastospores were then harvested by centrifugation (3273 ***g***, 4°C, 15 min), resuspended in water and stored on ice until infection (0–1 d). Their concentration was determined using Kova Glasstic counting chambers (Hycor Biomedical Inc., Garden Grove, CA, USA) and adjusted to concentrations of 10^6, 5 × 10^6 or 10^7 spores ml^{-1} in 0.1% Tween 20. Infection assays with wild-type strains were performed at a concentration of 10^6 spores ml^{-1}; assays with isogenic lines were performed at 10^6 and 5 × 10^6 spores ml^{-1}; and the confocal microscopy assay with *Z. ardabiliae* was performed at 10^7 spores ml^{-1}. The number of replicates per experiment is shown in Table S2.

Infection with *Z. pseudotritici* and *Z. ardabiliae* was performed on cultivar Runal. Blastospore suspensions were obtained as described before but grown in yeast-peptone-dextrose media (YPD; 10 g l^{-1} yeast extract, 20 g l^{-1} peptone, 20 g l^{-1} dextrose) for 6–8 d (18°C, 120 rpm). Concentrations were adjusted to 10^7 spores ml^{-1} in 0.1% Tween 20 before infection. Thirty milliliters of this suspension was used to spray-inoculate two pots containing 16–20 seedlings each. Pots containing inoculated plants were placed in plastic bags for 3 d as previously described (Meile *et al.*, 2018) to increase humidity. Inoculated plants were kept under the same conditions as before inoculation for experiments that included only Swiss strains or mutant strains derived from the Swiss strain 3D1. Whenever strains from Iran, Israel, Australia, or the USA were used, the inoculated plants were kept in a closed growth chamber (16 h photoperiod, 18°C : 15°C, day : night, 80% humidity). For the isogenic lines expressing different *Avr3D1* alleles, two to three independent transformants were analyzed in cultivar Runal (Fig. S3).

RNA isolation and quantitative reverse transcription PCR

RNA was obtained from *Z. pseudotritici*- and *Z. ardabiliae*-infected Runal plants and from axenic cultures grown in YPD. Ten days after infection, wheat leaves were harvested by removing 2 cm from the distal part of the leaf and flash-freezing the adjacent 10-cm section. Blastospores grown in YPD for 7 d were centrifuged at 4°C and frozen in N_2. RNA extraction was performed as described (Meile *et al.*, 2018), and cDNA synthesis was performed using GoScript Reverse Transcriptase Kit (Promega) from up to 1 µg RNA per reaction. Quantitative reverse transcription PCR was performed on a LightCycler 480 (Roche Diagnostics International AG). The 10-µl reactions contained each primer at 250 nM, 2.5 µl of cDNA and 1× HOT FIREPol EvaGreen qPCR Mix Plus mastermix (Solis BioDyne, Tartu, Estonia). We used the homologues of Actin (Mycgr3G105948) in *Z. pseudotritici* and *Z. ardabiliae* as reference gene (Table S1). We corrected for primer efficiency of each primer pair, which was calculated using LinRegPCR (Ruijter *et al.*, 2009). At least two technical replicates were assessed per sample. Raw data of the qPCR, which is included in Table S3, were processed using Rstudio v.11.2.1335 (RStudio Team, 2015).

Phenotyping and data analysis

Symptoms were quantified by mounting the second leaves on paper sheets with the adaxial side facing up, scanning them using a CanoScan LiDE 220 flatbed scanner (Canon Inc., Tokyo, Japan) with a resolution of 1200 dots per inch, and analyzing them with an ImageJ-based automated image analysis tool (Schneider *et al.*, 2012; Stewart *et al.*, 2016). The obtained phenotype data were processed using the ggplot2 package in Rstudio v.1.2.1335. Confidence intervals of the medians were estimated using the boot package and pairwise Wilcoxon rank sum statistical tests were performed using the stats package. Shapiro test was performed and showed that the data on pycnidia cm^{-2} and percentage of leaf area covered by lesions did not follow a normal distribution. Raw data can be found in Tables S3 and S4.

Confocal microscopy analysis

To visualize growth during host colonization of *Z. ardabiliae* and of *Z. tritici* expressing two different alleles of *Avr3D1* (*Avr3D1$_{3D1}$*, *Avr3D1$_{ISR398}$*), we used an inverted Zeiss LSM 780 confocal microscope (Carl Zeiss AG) using both DPSS (561 nm) and Argon (488 nm) lasers as illumination sources and an LD C-Apochromat ×40/1.1 W Korr m27 objective. We detected the following signals: eGFP (494.95–535.07 nm); plant autofluorescence (561.36–596.87 nm) and chloroplast autofluorescence (656.01–681.98 nm). Wheat seedlings (cultivar Runal) were infected with the GFP-expressing mutant lines 3D1Δ*avr3D1*, 3D1Δ*avr3D1* + *Avr3D1$_{3D1}$*, 3D1Δ*avr3D1* + *Avr3D1$_{ISR398}$* and *Z. ardabiliae* as described above. Infected second leaves were harvested. The top 3 cm of the leaves were discarded and adjacent sections of *c.* 2 cm were observed in 0.02% Tween 20 on the adaxial side. To estimate the penetration success rate, we specifically searched for fungal individuals growing on the leaf surface that were in close contact with stomata. Using the live search mode with various Z-positions of the confocal microscope, we determined whether each penetration event was successful or not. For each fungal mutant line, we observed three independent leaf sections and assessed between 16 and 21 individuals per leaf section. Images were acquired with Zeiss Zen Black 2012 software with a resolution of 1024 × 1024 pixels and processed using the Fiji platform of ImageJ v.2.0.0-rc-69/1.52p (Schneider *et al.*, 2012). Processing included pseudo-coloring, merging all channels, cropping, adjusting brightness and contrast, adding scale bars, and generating maximum intensity z-projections and orthogonal views. Tukey's HSD statistical test was performed using the stats package in Rstudio v.1.2.1335.

Protein sequence alignment, cladogram, and estimation of the effect of different amino acid substitutions

Protein sequences were aligned using CLC Genomics Workbench 11.0 (Qiagen; Gap cost = 10, gap extension cost = 1.0). The aligned isoforms of Avr3D1 were used to construct the Maximum Likelihood phylogeny using CLC Genomics Workbench 11.0 (Qiagen), using the Jukes–Cantor distance and 100 bootstrap replications. To quantify the different levels of avirulence caused by the different Avr3D1 isoforms, we assigned an avirulence category from 0 to 5 to each isoform (Fig. S4). If two isoforms led to a significantly different disease outcome as measured by the percentage of leaf area covered by lesions, they were assigned to different avirulence categories, with 0 indicating no detectable avirulence and 5 indicating the highest level of avirulence among all tested Avr3D1 isoforms. Due to the quantitative nature of the disease progression, differences between mutant lines can be temporal and only visible at specific time points. For example, if symptoms are measured at a stage of infection where most of the leaf area is necrotic, the differences in virulence might not be detected. For this reason, quantitative differences between mutant lines were not detected in all experiments, likely due to small differences in the glasshouse growing conditions. This was the case for the mutant expressing the ORE.R.a12.3B3 allele compared with 3D1Δ*avr3D1* and for 3D1Δ*avr3D1* + *Avr3D1$_{ISR8036}$* compared with 3D1Δ*avr3D1* + *Avr3D1$_{ORE.R.3B3}$*. In those cases, we considered that two isoforms were in different categories if they exhibited statistically different virulence phenotypes in at least half of the experiments. All strains with significant differences found in less than half of the experiments were classified into the same virulence category.

To find a possible correlation between sequence identity and difference in avirulence category, the mature sequences of Avr3D1 were aligned as described above, and pairwise sequence comparisons were performed in CLC Genomics Workbench 11.0 (Qiagen). A correlation plot was generated in Rstudio v.1.2.5042 (RStudio Team, 2015) using ggscatter and stat_cor from the ggpubr package. To estimate the contribution of each amino acid substitution to virulence differences, we calculated the average phenotypic effect of each substitution for each pairwise isoform comparison by dividing the difference in virulence

category by the number of amino acid substitutions. For each amino acid substitution, the average phenotypic effects for each pairwise isoform comparison were averaged over all pairwise comparisons in which the substitution occurred. A bar and dot plot was generated in RSTUDIO v.1.2.5042 using the GGPLOT2 package.

Computational analysis of protein structure

Secondary structure predicted from sequence was obtained with the PSIPRED webserver (Buchan & Jones, 2019). Because of the low similarity between Avr3D1 and proteins with experimental structure available in the Protein Data Bank, models of 3D1 and 3D7 isoforms of Avr3D1 were predicted using TRROSETTA (Yang et al., 2020). The structural models obtained had a confidence value of 0.71 and 0.69, respectively, on a 0–1 scale.

Molecular Dynamics (MD) simulations using the CHARMM 3.1 force field and the multicore CUDA version of NAMD 2.13 in a Tesla V100 GPU were performed on Avr3D1. Systems were immersed in periodic rectangular solvation boxes with a spacing distance of 15 Å around proteins and water molecules added according to the TIP3P model. Na^+ and Cl^- ions were added to counter the total charge of protein systems while providing 0.150 M salt concentration. The total number of atoms involved in these simulations was 19 132. The following set of calculations was performed: (1) optimization along 5000 conjugate gradient minimization steps; (2) equilibration of water for 100 ps in 2-fs time steps at 298 K and 1 atm with all atoms except those of water fixed; and (3) simulation runs during 100 ns keeping the same time steps (which involves 50 million steps for every simulation), in the isothermal–isobaric (NPT) ensemble. Langevin dynamics for T control and the Nosé-Hoover Langevin piston method for P control were used. Output results were stored every 25 000 steps and the trajectories were processed and analyzed with VMD 1.9.3. The secondary structure was identified using DSSP (CMBI v.3.1.2).

Poisson–Boltzmann electrostatic potentials were computed with the APBS plugin implemented in PYMOL 2.3.2 (Schrodinger LLC, 2015). Atomic charges and radii were assigned for all atoms with PDB2PQR server (Jurrus et al., 2018), using the AMBER parameter set. Molecular graphics were prepared and rendered with PYMOL 2.3.2 (Schrodinger LLC, 2015). Structural alignment was performed using FATCAT, a method that optimizes a flexible structural alignment of fragment pairs minimizing the number of rigid-body movements (twists) around pivot points (Ye & Godzik, 2003).

Results

Different Z. tritici strains carrying different alleles of Avr3D1 exhibit virulence differences in cultivar Runal

To explore the prevalence of Avr3D1-related host evasion, we assessed the virulence phenotypes of a set of 23 Z. tritici strains carrying 18 different Avr3D1 alleles (Meile et al., 2018) in wheat lines with varying abilities to recognize the Avr3D1 isoform of

the avirulent strain ST99CH_3D1 (3D1; Avr3D1$_{3D1}$). The wheat lines Runal, TE-9111, and ST6 had been shown to recognize Avr3D1$_{3D1}$ and are therefore referred to as resistant hosts, while the wheat lines Titlis and Drifter do not carry the corresponding resistance gene (Meile et al., 2018) and are therefore referred to as susceptible hosts. ST99CH_3D7 (3D7) is highly virulent in the three resistant and two susceptible hosts (Meile et al., 2018; Fig. 1b). Each strain was phenotyped on at least two resistant hosts and at least one susceptible host. A strain was considered avirulent on resistant hosts if it produced fewer symptoms than the virulent control strain 3D7 and considered virulent if symptoms were comparable to 3D7. On susceptible hosts, strains were considered avirulent if they produced fewer symptoms than both the control strains 3D7 and 3D1, which are both virulent on susceptible hosts. Strains were considered virulent if symptoms were similar or more severe compared to at least one of the control strains. Fifteen (65%) strains, including 3D7, were virulent on at least one resistant host (Fig. 1), suggesting that they are able to escape Avr3D1-triggered defense and carry virulent Avr3D1 alleles. These 15 strains harbored 13 different Avr3D1 isoforms. The remaining eight (34%) strains, including 3D1, were avirulent on all tested resistant hosts; however, three (13%) of them were also avirulent on the susceptible hosts (Fig. 1), suggesting that their overall virulence is generally low, regardless of a possible Avr3D1-triggered defense. Four (17%) strains were avirulent on all resistant hosts but virulent on susceptible hosts (Fig. 1), suggesting that they carry avirulent Avr3D1 alleles. We observed that in some cases strains expressing the same allele of Avr3D1 displayed different virulence phenotypes in certain hosts, highlighting that additional factors, such as effectors, other than Avr3D1, influence the virulence outcome of these wild-type strains. For example, the strains ST99CH_3A10 (3A10) and ST99CH_3F4 (3F4) had the same allele but gave opposite phenotypes. While 3A10 displayed behavior expected for an avirulent strain, 3F4 fully colonized the resistant cultivar Runal. Therefore, we could not conclude whether 3F4 and 3A10 harbor a virulent or an avirulent Avr3D1 isoform. Overall, we showed that there is considerable naturally occurring virulence variation, and the data suggest that evasion of Avr3D1 recognition is frequent in Z. tritici populations.

Different natural Avr3D1 isoforms lead to different magnitudes of pathogen infection

To determine whether mutations in the coding region of Avr3D1 caused escape from recognition, we eliminated Avr3D1-unrelated strain-to-strain differences by expressing different Avr3D1 alleles in isogenic mutant lines in the virulent genetic background of strain 3D1 lacking the Avr3D1 gene (3D1Δavr3D1). Ten different Avr3D1 isoforms were evaluated for their capacity to induce defenses in cultivar Runal, using transformant lines expressing Avr3D1$_{3D1}$, Avr3D1$_{3D7}$, and the mutant line 3D1Δavr3D1 as controls. The isoforms from the strains AUS_1E5 and AUS_1B1, in addition to Avr3D1$_{3D7}$, did not result in changes in virulence compared to 3D1Δavr3D1 (Fig. S5), suggesting that they are not recognized and are therefore considered virulent

(a)

| Strain	Resistant hosts			Susceptible hosts		Prediction
	Runal	ST6	TE-9111	Titlis	Drifter	
ST99CH_3D1	a	a	a	v	v	–
ST99CH_3B4	a	a	nd	a	nd	Not possible
ST99CH_3D7	v	v	v	v	v	
ST99CH_3A1	v	v	nd	v	a	Virulent
ST99CH_3A10	a	a	a	a	v	Not possible
ST99CH_3F4	v	nd	a	nd	v	
ST99CH_3A2	v	a	nd	v	nd	Virulent
ST99CH_3A5	v	v	nd	v	nd	Virulent
ST99CH_3A6	v	a	nd	v	nd	Virulent
ST99CH_3F1	v	a	v	v	v	Virulent
ST99CH_3F2	v	v	nd	v	nd	Virulent
ST99CH_3F3	a	a	v	a	v	Virulent
ST99CH_3D3	v	nd	v	nd	v	
ST99CH_3G6	v	v	nd	a	nd	Virulent
ST99CH_3H1	v	a	nd	v	nd	Virulent
ST99CH_3H4	v	v	nd	v	nd	Virulent
ISY_Ar_12d	a	a	nd	nd	a	Not possible
ISY_Ar_19e	a	a	nd	nd	a	Avirulent
ISY_Ar_21a	a	a	nd	nd	v	
ISY_Ar_16h	a	a	a	nd	v	Avirulent
ORE.S.a15 2A16	a	a	nd	nd	v	Avirulent
ORE.R.a12.3B3	a	v	nd	nd	v	Virulent
IPO323	v	v	nd	nd	v	Virulent

(b)
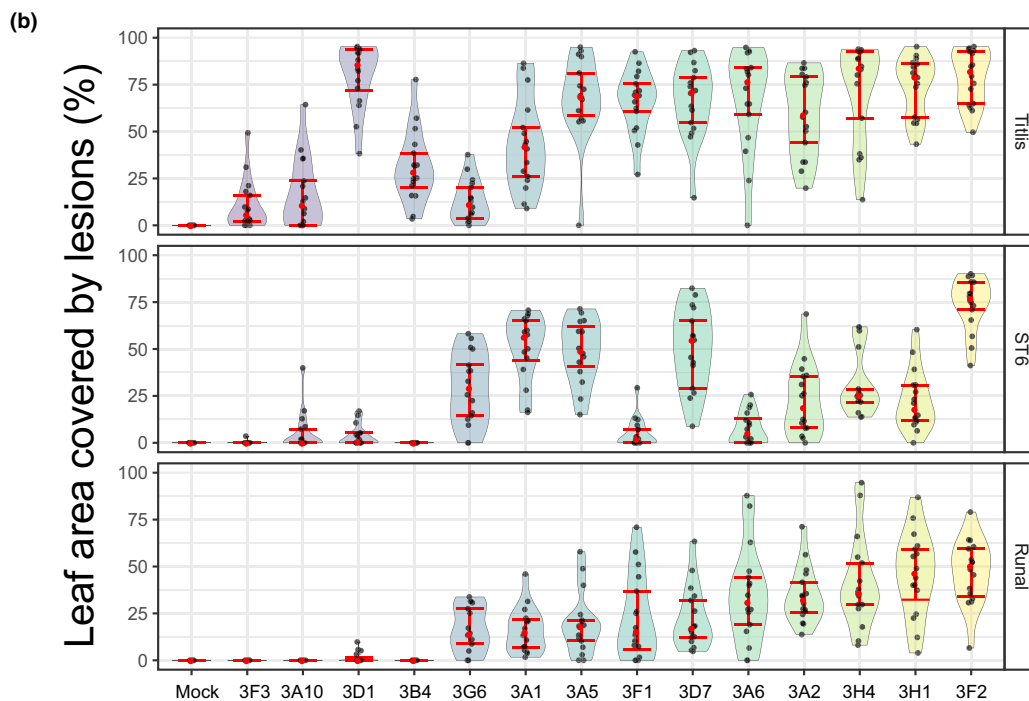
Fig. 1 The majority of *Zymoseptoria tritici* strains harboring different alleles of *Avr3D1* evade host recognition. (a) Twenty-three strains from different populations (ST99CH strains were from Switzerland, ISY_Ar from Israel, ORE from Oregon, AUS from Australia, IPO323 from the Netherlands) were assessed for cultivar-specific virulence using wheat lines either with (Runal, ST6 and TE-9111) or without (Titlis and Drifter) specific resistance triggered by the avirulence factor Avr3D1. Different background colors of the strain names indicate the presence of different isoforms of Avr3D1. In resistant wheat lines, strains were considered avirulent ('a', green background) if the percentage of leaf area covered by lesions (PLACL) was lower than for the virulent strain 3D7 and strains were considered virulent ('v', brown background) if lesions developed similarly or faster than in 3D7. In susceptible cultivars, strains were considered avirulent if the PLACL was lower than both 3D1 and 3D7 and considered virulent in any other case. Based on the virulence phenotype of the wild-type strains, predictions on whether they are likely to harbor a virulent or an avirulent isoform of Avr3D1 are indicated. Strains that were avirulent in all tested resistant and susceptible cultivars were not considered for predictions about Avr3D1 recognition. The PLACL was determined using automated image analysis and compared between strains using the pairwise Wilcoxon rank sum test ($\alpha = 0.01$). nd, not determined. (b) Violin plots showing the PLACL of wheat leaves (cultivars Titlis, ST6 and Runal) infected by Swiss strains of *Z. tritici*. Plants were phenotyped at 14 d post infection using automated image analysis. Red dots represent the median, error bars represent the 95% confidence interval of the median, and gray dots represent the individual data points. Sixteen biological replicates were collected for each treatment.

isoforms. Eight isoforms that led to a reduction in symptoms compared with 3D1Δ*avr3D1* (Fig. S4) were recognized by the resistant cultivar, and therefore considered to be avirulent isoforms. Interestingly, the reduction in virulence was not the same for all the tested isoforms. Isoforms from ORE.R.a12.3B3 (Avr3D1$_{ORE.R\_3B3}$), ISR8036 (Avr3D1$_{ISR8036}$), 3F4 (Avr3D1$_{3F4}$), and AUS_1A6 (Avr3D1$_{AUS\_1A6}$) led to a slight reduction in symptoms compared with the virulent control and a smaller reduction in symptoms than Avr3D1$_{3D1}$, while isoforms of the strains ISY_Ar_19e, IPO87019, ISY_Ar_16h, and ISR398 (Avr3D1$_{ISY\_Ar\_19e}$, Avr3D1$_{IPO87019}$, Avr3D1$_{ISY\_Ar\_16h}$ and Avr3D1$_{ISR398}$, respectively) reduced symptoms even more than Avr3D1$_{3D1}$ (Figs 2, S4). These highly avirulent Avr3D1 isoforms also led to a reduction in pycnidia formation (Figs S4, S6). Remarkably, no tested isoform completely abolished symptom development or formation of pycnidia (Figs 2, S4, S6), suggesting that the quantitative nature of the defense response is a general feature of Avr3D1 recognition. In total, we were able to distinguish five statistically different levels of resistance triggered upon recognition of the different isoforms of Avr3D1. Accordingly, we assigned an avirulence category to each isoform (Figs 2, S4), with 'stronger' avirulence alleles triggering a stronger host response that leads to fewer symptoms than 'weaker' avirulence alleles.

We also investigated whether the quantitative nature of Avr3D1 recognition was cultivar-specific by analyzing the virulence of five Avr3D1-expressing isogenic lines on the resistant wheat lines ST6 and TE-9111. Strong and weak avirulence alleles of *Avr3D1* triggered quantitative resistance responses on both resistant cultivars comparable to those observed on Runal (Fig. S6). On the contrary, all the investigated isogenic lines exhibited high virulence on the susceptible cultivar Drifter (Fig. S6). Altogether, we demonstrated that different magnitudes of resistance are triggered by different Avr3D1 isoforms in the three resistant wheat cultivars.

Avirulence is associated with a quantitative decrease in penetration success

To assess the impact of Avr3D1 recognition on microscopic disease progression and to test whether this impact is also quantitative in nature, we monitored the growth of isogenic lines expressing two Avr3D1 isoforms exhibiting different degrees of recognition. All the investigated mutant lines grew as characteristic spreading hyphae on the leaf surface. However, the expression of *Avr3D1$_{3D1}$* and *Avr3D1$_{ISR398}$* led to a decrease in penetration efficiency as measured by the percentage of fungal individuals in contact with host stomata that not only grew epiphytically but also apoplastically at 6 dpi (Fig. 3; Videos S1–S4). In accordance with the quantitative symptom reduction, the expression of the stronger allele *Avr3D1$_{ISR398}$* led to a lower penetration rate than the isogenic line expressing the weaker avirulence allele *Avr3D1$_{3D1}$*. These data suggest that Avr3D1 recognition occurs at early stages of the infection, before or during stomata penetration and that penetration efficiency is, similarly to virulence, a quantitative trait that is governed by Avr sequence polymorphisms.
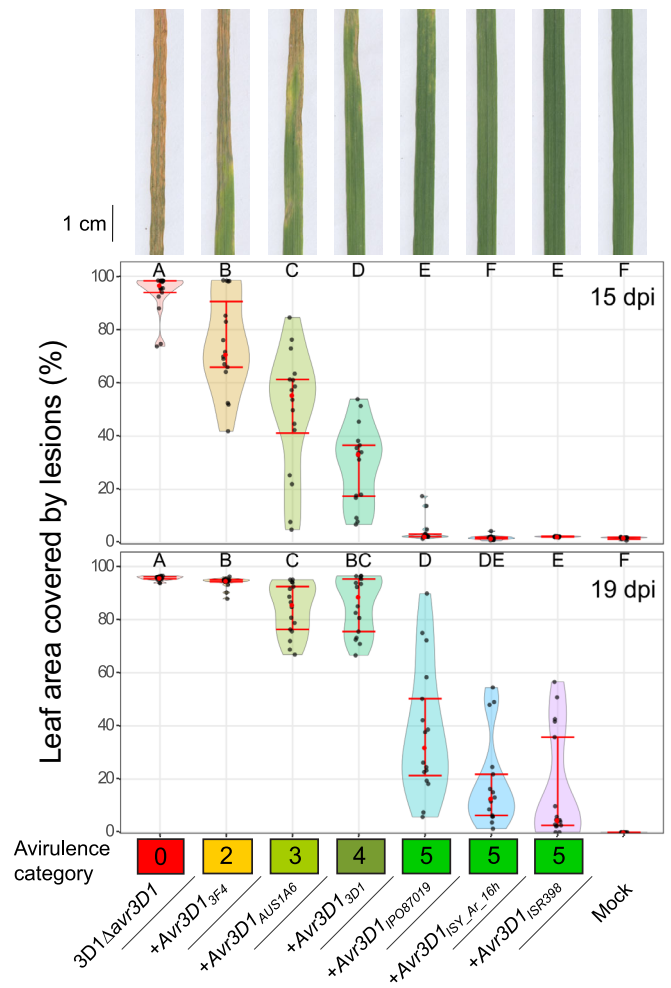

Fig. 2 Different isoforms of Avr3D1 lead to different magnitudes of pathogen infection. Top panel: representative images of wheat leaves (cultivar Runal) infected with *Zymoseptoria tritici* strain 3D1 lacking *Avr3D1* (3D1Δ*avr3D1*) and the same strain harboring an ectopic copy of different alleles of *Avr3D1* (+*Avr3D1$_{strain\ name}$*) at 15 d post infection (dpi). Lower panels: violin plots showing the percentage of leaf area covered by lesions (PLACL) of wheat leaves infected with the same *Z. tritici* isogenic lines. Plants were phenotyped at 15 (top and middle panels) and 19 (bottom panel) dpi using automated image analysis. Red dots represent the median, error bars represent the 95% confidence interval of the median and gray dots represent the individual data points. Sixteen biological replicates were collected for each treatment and time point, except for the mock infection treatment, which consisted of eight biological replicates. Letters along the top indicate statistical groups according to the pairwise Wilcoxon rank sum test ($\alpha = 0.01$). Bar, 1 cm. The resulting avirulence category of each isoform is shown in colored boxes with different colors indicating different avirulence categories.

Several mutations in *Avr3D1* underlie evasion of host recognition

To identify candidate residues in Avr3D1 that could be responsible for host evasion, we aligned 33 different isoform sequences identified in 135 strains isolated from five countries, setting the highly avirulent isoform ISY_Ar_19e as a reference. We colored each isoform based on their avirulence category and each amino
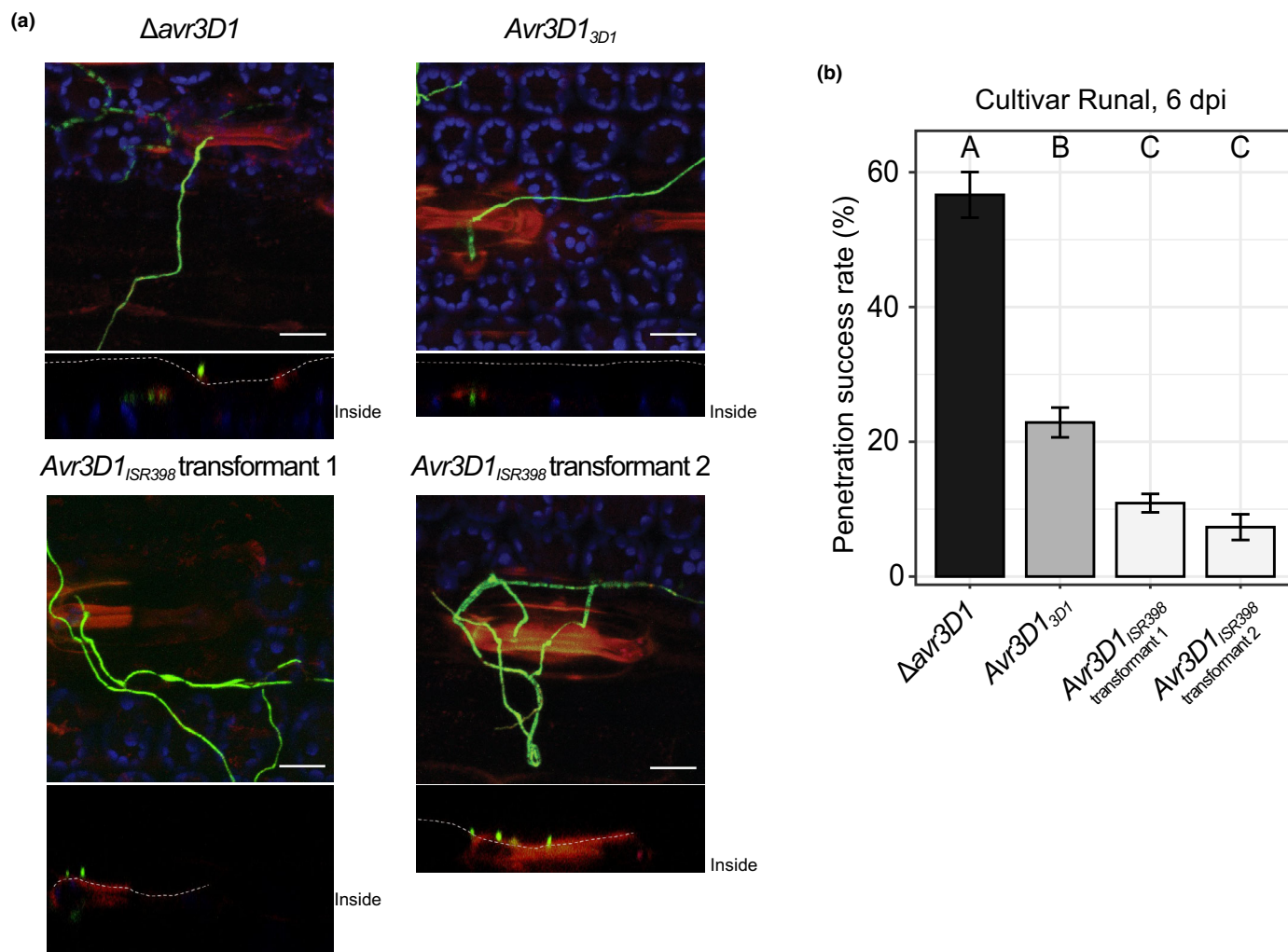
Fig. 3 Growth inside host leaf tissue is hindered in a quantitative manner in strains expressing avirulent alleles of *Avr3D1*. (a) Confocal laser scanning microscopy images of isogenic GFP-tagged *Zymoseptoria tritici* mutant lines expressing either *Avr3D1*$_{3D1}$, *Avr3D1*$_{ISR398}$ or no *Avr3D1* (Δ*avr3D1*) while in contact with wheat (*Triticum aestivum*) stomata. Green indicates the GFP detection channel, blue indicates chloroplast autofluorescence and red indicates leaf autofluorescence. Pictures were taken at 6 d post infection. Two independent transformants are shown for the mutant line expressing *Avr3D1*$_{ISR398}$. In the picture taken of transformant 1, a rare event of successful penetration is shown. In the picture shown for transformant 2, penetration was not successful. Maximum projection and orthogonal views are shown. Bars, 20 μm. The serrated lines in the orthogonal view approximately indicate the leaf surface. (b) Stomata penetration success rate of the strains shown in (a). Bars show the mean of three biological replicates consisting of 16–22 observations each and error bars show the SE of the mean. Letters above bars indicate statistical groups based on Tukey's HSD test ($\alpha = 0.05$).

acid substitution based on the avirulence category of the most avirulent isoform in which the substitution occurred. We identified 12 amino acid substitutions that occurred in highly avirulent isoforms (Fig. 4). These mutations were probably not involved in preventing recognition by the host. We identified nine additional substitutions that were unique to isoforms that completely escaped recognition. These nine substitutions represent high-priority candidate mutations for host evasion (Fig. 4a; A21G, 22insR, 24insV, P31S, H32D, A34K, H36N, I44T, Q75K; highlighted in red). Virulent isoforms harbored between two and three of these high-priority candidate mutations. Avr3D1$_{3D1}$ and Avr3D1$_{AUS\_1A6}$ exhibited a slight difference in triggering defense and the only amino acid substitution between them is G86W, which explains their quantitative phenotypic difference (Fig. 4a). We also investigated whether differences in the overall amino

acid sequence provided a good estimation of phenotypic differences. We did not observe a correlation between phenotypic differences, based on the avirulence category, and percentage of sequence identity in pairwise comparisons (Fig. 4b). In accordance, avirulent isoforms did not group together in a phylogenetic tree, and we identified two different clades with highly avirulent isoforms (Figs 4a, S7). Remarkably, we also observed three different virulent isoforms that were distantly related (Figs 4a, S7), suggesting that escape from recognition occurred independently at least three times.

In order to quantitatively estimate the impact of each mutation on host evasion, we performed pairwise comparisons of virulence categories for all tested Avr3D1 isoforms, normalized this value to the number of total substitutions per pair and calculated the average for all pairwise comparisons in which a substitution
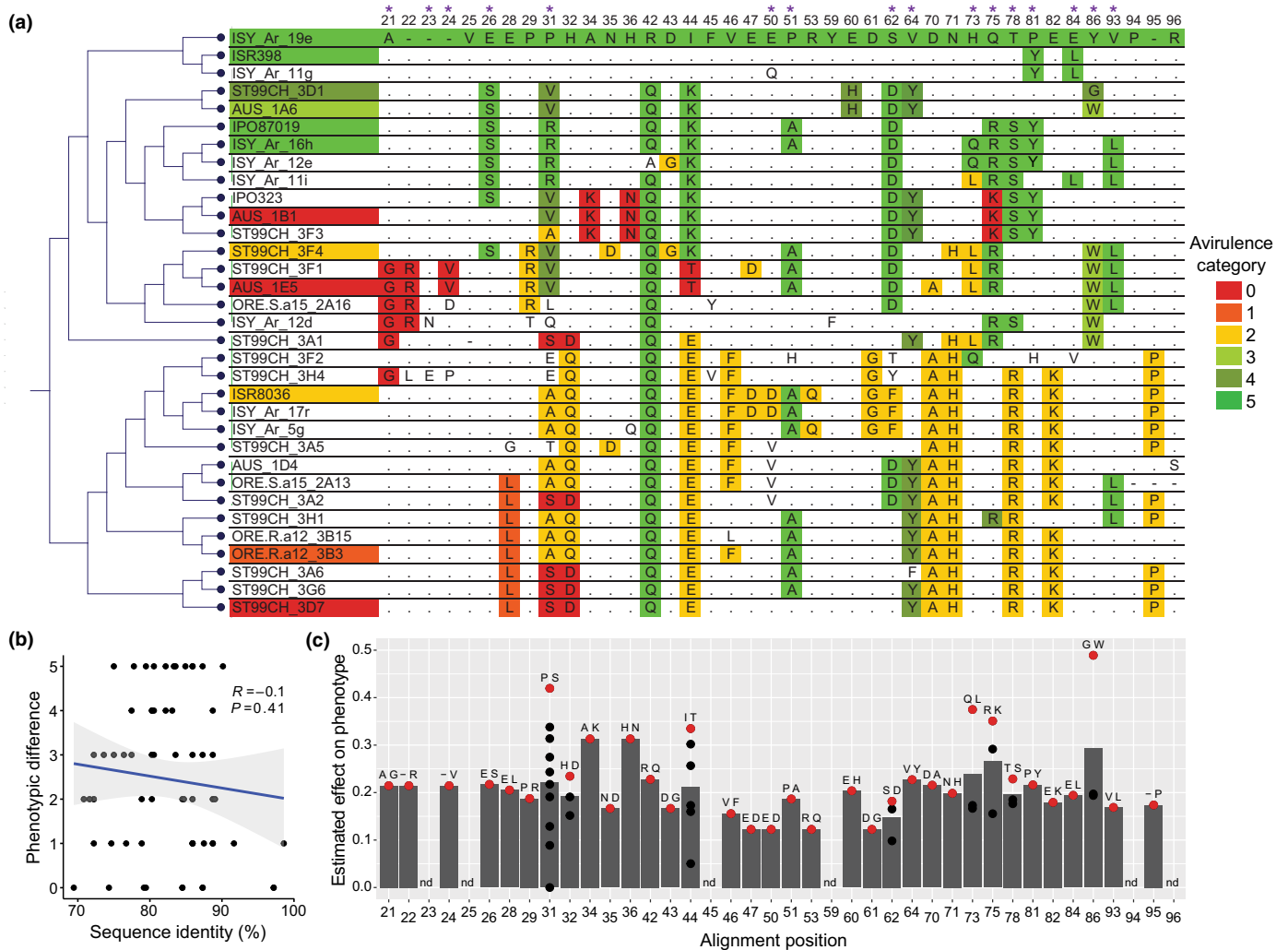
(a)

(b)

(c)

Fig. 4 Several amino acid substitutions in Avr3D1 are associated with host evasion. (a) Maximum likelihood tree and alignment of 33 Avr3D1 isoforms identified in 135 *Zymoseptoria tritici* strains. Fully conserved residues are not shown and residues that are identical to the isoform of strain ISY_Ar_19e are represented as a dot. Isoform names are color-coded based on their avirulence phenotype category, ranging from 0 (highly virulent, red) to 6 (highly aviru-lent, green). Amino acid substitutions compared with ISY_Ar_19e are color-coded based on the avirulence category of the most avirulent isoform in which the substitution occurred. Numbers indicate the position of the alignment and purple asterisks in the top row indicate residues that had previously been shown to be under significant diversifying selection (Meile *et al.*, 2018). (b) Pearson correlation plot between the percentage of sequence identity of the mature Avr3D1 protein and the virulence phenotype of all pairwise Avr3D1 isoform comparisons. Black dots represent the pairwise comparisons and the blue line indicates the regression line. (c) Estimated effect of different amino acid substitutions on the avirulence phenotype category based on pairwise comparisons of all tested Avr3D1 isoforms. Black dots indicate the estimated phenotypic effect of different amino acid substitutions averaged over all pair-wise comparisons in which the substitutions occurred. Red dots indicate the amino acid substitution with the highest estimated phenotypic effect for each residue averaged over all pairwise comparisons in which the substitution occurred. Gray bars indicate the mean estimated phenotypic effect of all substitutions occurring at a given residue. nd, not determined.

occurred. Based on this analysis, G86W was identified as the sub-stitution with the highest estimated phenotypic effect for all the analyzed substitutions. The substitution with the second highest estimated effect on virulence was P31S. This substitution occurred in the virulent strain 3D7. At this residue, two other substitutions also exhibited a high estimated effect (R31V and R31S). Additionally, mutations A34K, H36N, I44T, Q73L, and R75K had a high estimated effect on the virulence phenotype (Fig. 4c). We therefore considered these substitutions to be can-didate mutations that most likely contributed to gradual escape from Avr3D1 recognition and, consequently, to quantitative resistance triggered by Avr3D1. The four candidate residues

involved in host evasion featuring the highest estimated pheno-typic effects (31, 73, 75, and 86) were previously identified to be under positive diversifying selection (Meile *et al.*, 2018), indicat-ing that positive selection acting on *Avr3D1* was a key driver of escape from recognition (Fig. 4a,c).

Different regions in the three-dimensional structure of Avr3D1 are involved in host evasion

Having identified candidate residues involved in Avr recognition, we aimed to determine the structural basis of host evasion. The secondary structure of the 3D1 isoform of Avr3D1 consisted of

one 3_{10}-helix (residues 34–36), one α-helix (residues 38–48), and two antiparallel β-strands (residues 55–58 and 62–65), stabilized by four disulfide bridges (C33–C56, C41–C65, C38–C92, and C40–C88; Fig. 5a). Interestingly, sequence differences between 3D1 and 3D7 did not lead to global changes in the 3D structure of Avr3D1 (Fig. S8). The charge distribution, computed by the Poisson–Boltzmann (PB) electrostatic potential, was not uniform over the protein surface, featuring an extended region with negative potential and a smaller one, including the N- and C-terminal ends, displaying positive potential (Fig. 5b). The seven candidate residues involved in host evasion were located in spatially distant regions of the protein. Five of these residues were located in coil secondary structure, and none of them were in the β-strands or in the large electronegative region (Fig. 5a). The hydrophobic core, containing the disulfide bridges, was able to maintain the structure of the protein along the Molecular Dynamics (MD) simulation. By contrast, the N-terminal end of the protein is characterized by a significantly higher mobility. Three of the identified candidate residues were located in this high-mobility region (Fig. 5c). The structural analysis revealed that different regions of the 3D structure of Avr3D1 are involved in host recognition (Fig. 5a).

Homologues of Avr3D1 from different *Zymoseptoria* species trigger resistance in wheat

To explore the diversity of Avr3D1 across the species boundary, we investigated the presence of homologues of Avr3D1 in related *Zymoseptoria* species that are nonpathogenic in wheat. Using BLAST, we identified two homologues of Avr3D1 each in *Z. ardabiliae* and *Z. pseudotritici* but none in *Z. brevis* and *Z. passerinii*. An additional homologue was identified in *Z. tritici* on chromosome 5 (Figs S1, S9). The closest homologues in *Z. ardabiliae* and *Z. pseudotritici* shared 53.4% and 60.2% protein sequence
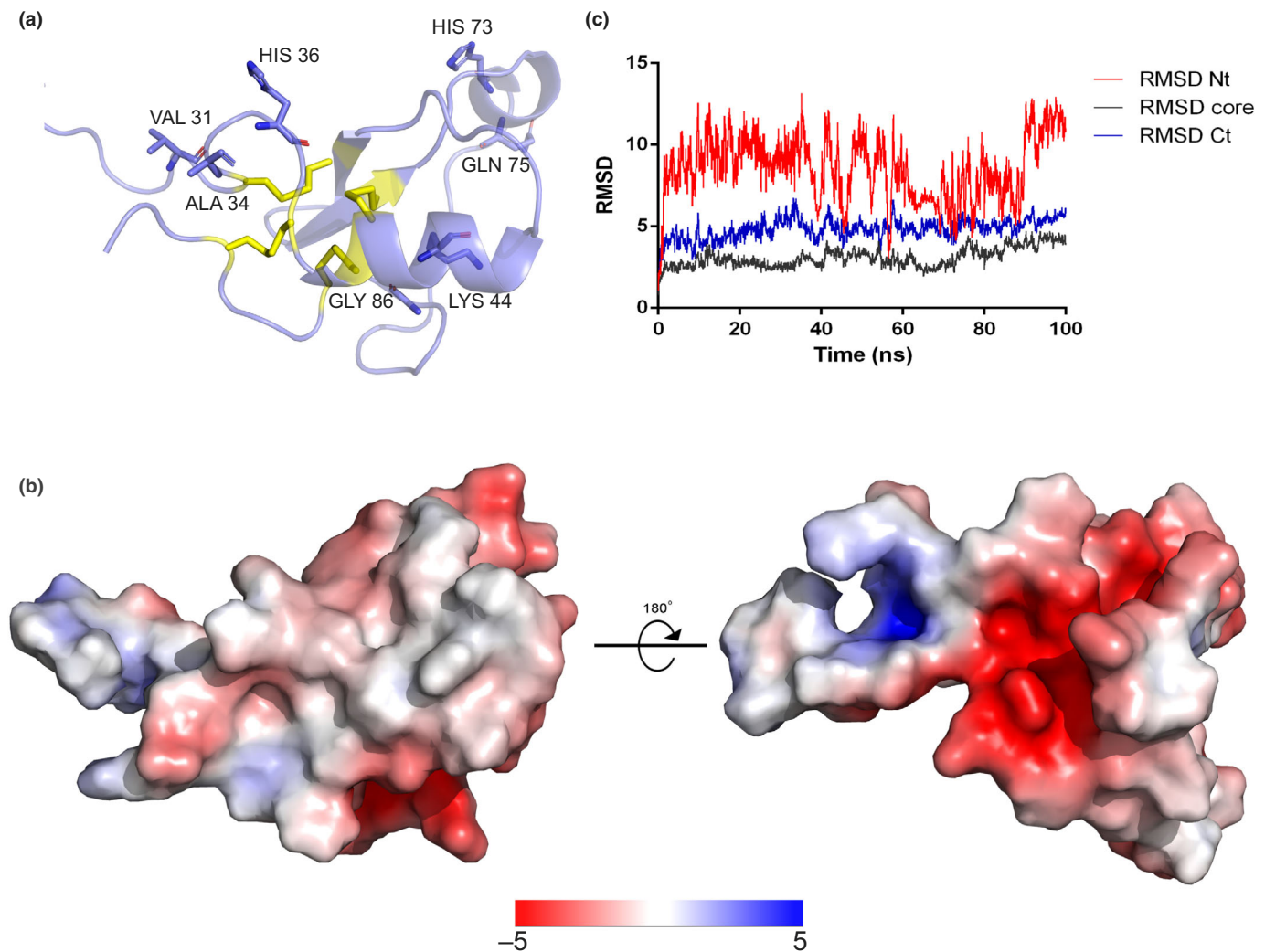

Fig. 5 Candidate residues mediating recognition are located in different locations in the 3D structure of Avr3D1. (a) Ribbon diagram of the *Zymoseptoria tritici* Avr3D1 model obtained using TrRosetta, depicting the disulfide bonds as yellow sticks and the candidate residues involved in recognition as blue sticks. (b) Poisson–Boltzmann electrostatic potential mapped onto the outer surface of Avr3D1 with ionizable side chains at protonation states corresponding to pH 7.0. (c) Molecular Dynamics simulation of the N-terminal (Nt; residues 24–37, red), core (residues 38–74, black) and C-terminal (Ct; residues 75–95, blue) regions. Root-mean-square deviation (RMSD) of the protein backbone as a function of time.

identity with Avr3D1$_{3D1}$, respectively. In *Z. pseudotritici*, the closest homologue (ZpAvr3D1) was found in all five investigated strains and its protein sequence was fully conserved. The closest homologue in *Z. ardabiliae* (ZaAvr3D1) was also found in all investigated strains, present as two different isoforms with a sequence identity of 98% and a frequency of 50% each (Meile *et al.*, 2018). Despite the relatively low sequence identity shared with Avr3D1, all cysteine residues were conserved in ZpAvr3D1 and ZaAvr3D1 (Figs 6c, S9). In addition, *in silico* signal peptide and effector predictions revealed that both homologues are likely to be secreted and to act as effectors.

To study whether Avr3D1 homologues are recognized in wheat, we investigated whether *Avr3D1* homologues from *Z. pseudotritici* and *Z. ardabiliae* were expressed during wheat infection. Remarkably, in both cases, there was an induction of *Avr3D1* expression *in planta* compared to axenic conditions (Fig. 6a). Furthermore, similar to an R-Avr interaction, the non-adapted pathogen *Z. ardabiliae* was able to grow on the leaf surface of wheat seedlings and exhibited unsuccessful attempts of stomata penetration (Figs 3, 6b). Next, we sought to test whether the homologues of Avr3D1 found in related *Zymoseptoria* species trigger defense in cultivar Runal. We expressed *ZpAvr3D1* and *ZaAvr3D1* in the virulent *Z. tritici* mutant line 3D1Δ*avr3D1*. Both homologues triggered a defense response in cultivar Runal (Fig. 6d), with ZaAvr3D1 leading to fewer symptoms than Avr3D1$_{3D1}$ (Fig. S10). Contrary to what we expected, the virulence of the mutants expressing the homologues of Avr3D1 on the resistant cultivar ST6 was not impaired (Figs 6d, S10), suggesting that none of the homologues were recognized by this cultivar. By contrast, in the susceptible cultivar Drifter, which does not recognize Avr3D1$_{3D1}$, both homologues led to a reduction in symptoms (Figs 6d, S10), indicating that they triggered an immune response. These results indicate that the *Z. ardabiliae* and *Z. pseudotritici* homologues of the avirulence factor Avr3D1 are recognized by wheat in a cultivar-specific manner, with distinct wheat lines able to recognize the homologues and Avr3D1 from *Z. tritici*, respectively. Overall, the data show that a resistance response can be induced by effectors of the nonpathogenic species *Z. pseudotritici* and *Z. ardabiliae* on wheat, indicating that Avr3D1 acts as a determinant of host specificity.

Discussion

Quantitative resistance, understood here as any resistance that is incomplete in an agricultural ecosystem (Cowger & Brown, 2019), has typically been considered to be mediated by mechanisms other than gene-for-gene interactions. By assessing the contribution to virulence of a panel of naturally occurring isoforms of a single Avr, we demonstrated that evasion of *R* gene recognition can lead to a gradation of resistance phenotypes instead of the binary phenotype typically associated with gene-for-gene interactions. We thus provide compelling evidence that gene-for-gene interactions are a major mechanism underlying quantitative resistance.

Recognition of avirulence factors triggering quantitative resistance phenotypes have rarely been investigated in filamentous pathogens using functional tools (Poland *et al.*, 2009; Niks *et al.*, 2015). In *Leptosphaeria maculans*, recognition of an avirulence factor expressed during late systemic colonization was shown to trigger quantitative resistance (Jiquel *et al.*, 2021). In *Pyricularia oryzae*, quantitative differences in virulence between two isolates were shown to be mediated by a gene-for-gene interaction (Zenbayashi-Sawata *et al.*, 2005). In both cases, only a single allele was investigated. In the effector Avr-Pik from *P. oryzae*, a single point mutation occurring in a wild isolate changed the magnitude of the induced resistance response (Maqbool *et al.*, 2015), indicating the quantitative nature of Avr-Pik-mediated resistance. Our comprehensive analysis of a wide variety of natural Avr isoforms demonstrates that even a single *Avr* gene can underlie a broad range of quantitative resistance phenotypes in an isoform-dependent manner. Remarkably, the quantitative nature of Avr3D1 recognition was observed in different wheat lines harboring Stb7 (TE9111 and ST6). We observed that the candidate residues involved in recognition are located in different positions of the primary and tertiary structures of the Avr3D1 protein. Similar scenarios were described for the avirulence factors AvrL567 in flax rust and ATR1 in *Hyaloperonospora arabidopsidis*, in which mutations associated with differential recognition were located in different positions of the proteins (Wang *et al.*, 2007; Chou *et al.*, 2011; Ravensdale *et al.*, 2012). The scattered recognition surface of Avr3D1 might provide a mechanistic explanation of why different isoforms lead to different magnitudes of quantitative resistance, since some regions of the R-Avr recognition surface might contribute more to the overall interaction than others. 3D modeling of different isoforms of Avr3D1 suggests that it is unlikely that major changes in the 3D structure are responsible for the escape from recognition. Additionally, we cannot discard that the observed phenotypes are due to differences in the protein stability of the different Avr3D1 variants, which would directly contribute to the magnitude of recognition.

We tested different wheat lines with and without *Stb7*, the most probable resistance gene against Avr3D1$_{3D1}$, for resistance against a panel of wild-type *Z. tritici* strains carrying different alleles of *Avr3D1*. The wild-type strains are genetically different and do not only differ in the sequence of *Avr3D1*, but also in the content of additional effectors. Therefore, the virulence phenotype of the wild-type strains was not exclusively due to Avr3D1 recognition, as confirmed by differences in virulence of wild-type strains harboring the same allele of *Avr3D1*. However, this experiment enabled us to identify potential avirulent isoforms of Avr3D1 and the prevalence of host evasion. Among the 16 investigated Swiss strains, only three were found to be avirulent on all tested wheat lines harboring the resistance gene, suggesting that host evasion of Avr3D1-triggered immunity is frequent in Swiss populations of *Z. tritici*. Remarkably, the strain 3F4 is virulent in Runal but harbors a weakly avirulent allele of *Avr3D1*. Therefore, Avrs may still contribute to quantitative resistance in apparently virulent strains, especially if the magnitude of Avr-triggered defense is on the low side of the spectrum, highlighting the importance of maintaining even apparently eroded *R* genes in breeding programs.

In previous work, we showed that *Avr3D1* is highly polymorphic in natural populations of *Z. tritici* (Meile *et al.*, 2018). Here, we demonstrate the prevalence of host evasion and show that at least three highly virulent isoforms arose independently. The independent emergence of virulent isoforms was not geographically restricted, two being identified in the Australian population and one in the Swiss population, providing evidence for the convergent evolution of host evasion. Although we could show that many natural Avr isoforms partially escaped recognition, several residues under diversifying selection were not
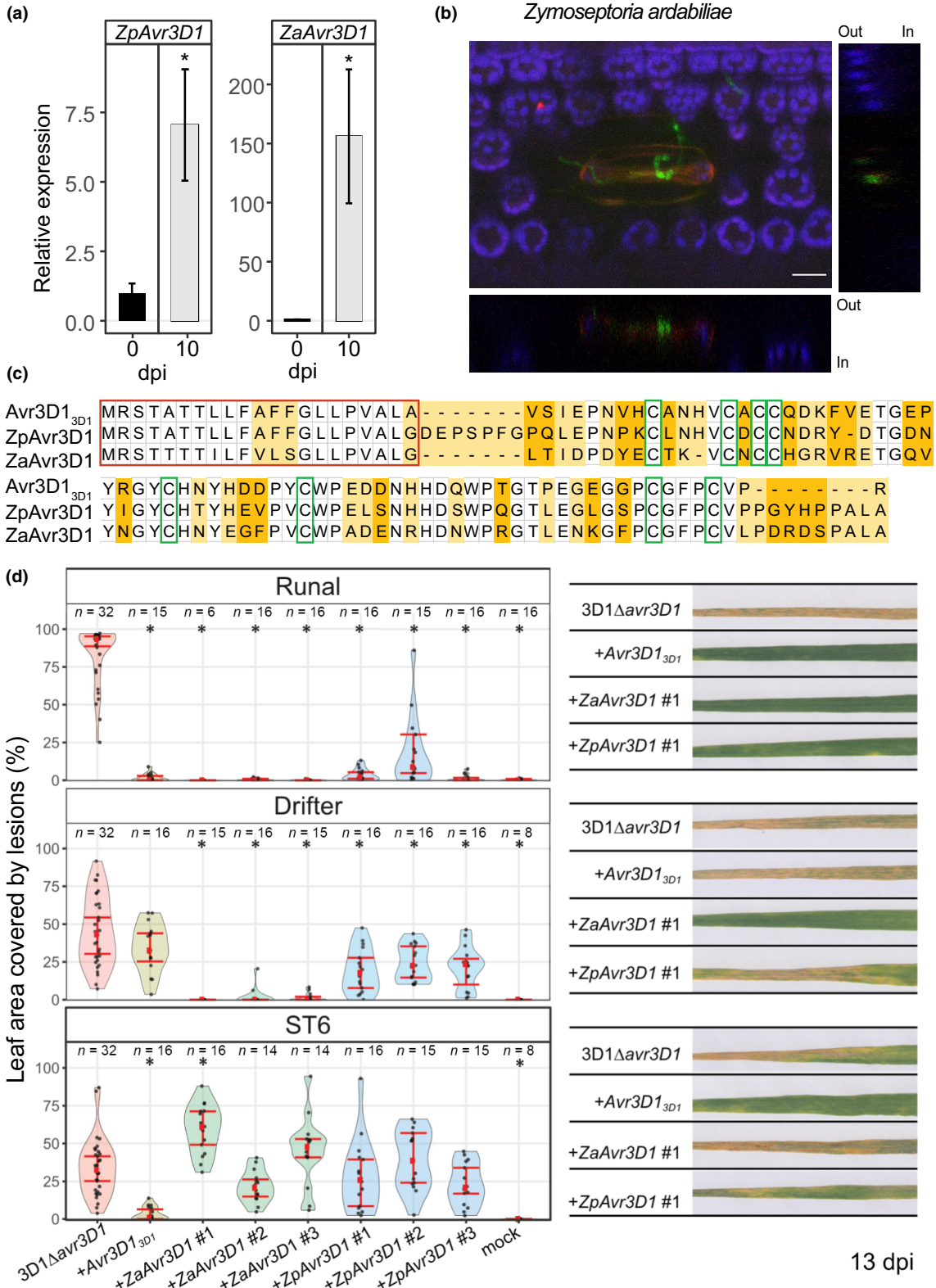
© 2022 The Authors
New Phytologist © 2022 New Phytologist Foundation.

Fig. 6 Homologous candidate effectors of closely related *Zymoseptoria* species trigger defense in wheat. (a) Relative expression of the homologues of *Avr3D1* in *Zymoseptoria ardabiliae* strain 2.2.1 (*ZaAvr3D1*) and *Zymoseptoria pseudotritici* strain 1.1.1 (*ZpAvr3D1*) in axenic medium and 10 d post infection (dpi) of wheat plants. Values are relative to 0 dpi. Error bars represent the SE of the mean. Asterisks represent statistical differences (Student's *t*-test, $\alpha = 0.05$). (b) Confocal laser scanning microscopy images of GFP-tagged *Z. ardabiliae* while in contact with host stomata. Green indicates the GFP detection channel, blue indicates chloroplast autofluorescence and red indicates leaf autofluorescence. Pictures were taken at 11 dpi. Maximum projection and orthogonal views are shown. Bar, 20 µm. (c) Protein alignment of Avr3D1 from *Zymoseptoria tritici* strain 3D1, *Z. ardabiliae* strain 2.2.1 and *Z. pseudotritici* strain 1.1.1. The predicted signal peptide position is indicated with a red box and cysteines with a green box. Sequence differences are indicated in dark yellow when the three sequences are different or light yellow when two of the sequences have the same amino acid. (d) Left: violin plots showing the percentage of leaf area covered by lesions at 13 dpi of cultivars Runal, Drifter and ST6 infected with *Z. tritici* strain 3D1 lacking *Avr3D1* (3D1Δ*avr3D1*) and isogenic lines expressing the *Avr3D1* allele from strain 3D1 (*Avr3D1₃D₁*) or the closest homologue from *Z. pseudotritici* or *Z. ardabiliae* (*ZpAvr3D1* and *ZaAvr3D1*, respectively). For *ZpAvr3D1* and *ZaAvr3D1*, three independent transformant lines are shown (#1, 2, 3). Red dots represent the median, error bars represent the 95% confidence interval of the median, and gray dots represent individual data points. The number of biological replicates (*n*) is shown. Black asterisks indicate statistical differences with 3D1Δ*avr3D1* according to the pairwise Wilcoxon rank sum test ($\alpha = 0.01$). Right: pictures of representative infected leaves for each treatment. The distal 5 cm of each infected leaf is shown.

identified as candidate residues for host evasion in our phenotype-based analysis. For example, the most frequent amino acids at the positively selected position 62 are D and S, both of which are present in virulent and avirulent isoforms. Avr evolution is not only driven by host recognition, but also by effector function optimization (Sánchez-Vallet *et al.*, 2018). Potentially, some of the identified mutations in residues under diversifying selection might have arisen to optimize Avr3D1-facilitated host colonization. An alternative explanation for mutations that are apparently unrelated to host evasion is that selection on Avr proteins might counteract a trade-off between escape from recognition and effector function. In cases where the effector function is disturbed by the alteration of residues critical for recognition, compensatory mutations may be selected to preserve or restore effector function, as hypothesized for AvrStb6 (Brunner & McDonald, 2018) in *Z. tritici* and AvrPm3 in *Blumeria graminis* f.sp. *graminis* (McNally *et al.*, 2018). These compensatory mutations would also exhibit positive selection, even though they were not selected to avoid host recognition. Since Avr3D1 is highly diverse, it will provide a valuable model to investigate the trade-off between escape from recognition and effector function optimization once its effector function is determined. Furthermore, we cannot discard the possibility that positively selected residues arose to avoid recognition in wheat genotypes that have not been tested in this study. This might be due to one or more different resistance genes or different alleles of the same unknown resistance gene. In line with this possibility of multiple *R* genes or alleles recognizing Avr3D1, we demonstrated that the cultivar Drifter, which is unable to recognize the tested Avr3D1 isoforms of *Z. tritici*, recognizes the homologues in *Z. pseudotritici* and *Z. ardabiliae*.

Zymoseptoria ardabiliae and *Z. pseudotritici* were isolated from wild grasses and are incapable of infecting wheat (Stukenbrock *et al.*, 2007). By contrast, *Z. tritici* is highly adapted to wheat (Stukenbrock *et al.*, 2007). The molecular mechanisms involved in host adaptation and speciation of *Z. tritici* are largely unknown, but it has been suggested that fixation of adaptive substitutions in genes involved in interactions with specific hosts played a major role (Stukenbrock *et al.*, 2011; Poppe *et al.*, 2015). Here, we showed that the closest homologues of Avr3D1 from *Z. ardabiliae* and *Z. pseudotritici* induce a strong defense response in wheat, suggesting their contribution to host range. As expected for a gene-for-gene relationship, the immune response triggered by Avr3D1

homologues was cultivar-specific. This finding is in accordance with the emerging idea that Avrs play a role in nonhost resistance (Schulze-Lefert & Panstruga, 2011; Ayliffe & Sørensen, 2019). We hypothesize that the closely related *Zymoseptoria* species harbor several Avrs, including Avr3D1, that concertedly abolish wheat infection. Avr recognition also plays a key role in host species specificity in *B. graminis* (Bourras *et al.*, 2019) and in specialization of the rice blast fungus to *japonica* and *indica* rice varieties (Liao *et al.*, 2016). Loss of an avirulence factor was proposed to facilitate the emergence of wheat blast (Inoue *et al.*, 2017). Here, we provide further support for the role of Avrs in determining a pathogen's host range. Hence, wheat *R* genes might not only represent a valuable resource to reduce the impact of current diseases, but also to prevent the emergence of new diseases.

Quantitative resistance against fungal pathogens has historically been exploited in crop breeding to achieve sustainable food production (Cowger & Brown, 2019). In this work, we demonstrate that the mechanisms underlying host range, qualitative resistance, and quantitative resistance are not exclusive. Overall, the findings that gene-for-gene interactions can lead to minor differences in virulence phenotypes opens the possibility that quantitative resistance in fungal pathosystems is based largely on repertoires of *Avr* and *R* genes with minor, additive effects that act in concert to govern compatibility.

Competing interests

None declared.

Author contributions

LM and AS-V contributed to the conceptualization and design of the work, acquisition and analysis of data and writing of the manuscript. MG-A obtained the structural models, prepared figures and contributed to the writing. ZB, JP, AS, AB and JA contributed to design experiments and data acquisition. BAM contributed to the conceptualization of work, writing and revision of the manuscript. MG-A, ZB and JP contributed equally to this work.

ORCID

Alessio Bernasconi https://orcid.org/0000-0003-3833-288X
Zoe Bernasconi https://orcid.org/0000-0002-1216-6791
María Garrido-Arandia https://orcid.org/0000-0001-6114-5754
Bruce A. McDonald https://orcid.org/0000-0002-5332-2172
Lukas Meile https://orcid.org/0000-0002-2680-3309
Andrea Sánchez-Vallet https://orcid.org/0000-0002-3668-9503

Data availability

The authors declare that the source data for Figs 1–6, S3–S6, and S10 have been provided in the Supporting Information. The genomic data of *Z. passerinii* (NCBI genome accession no. AFIY01 (fungal strain SP63)), four strains of *Z. ardabiliae* (STIR04 1.1.1 (accession no. AFIU01), STIR04 1.1.2 (AFIV01), STIR04 3.13.1 (AFIW01), STIR04 3.3.2 (AFIX01)), one strain of *Z. brevis* Zb18110 (LAFY01) and five strains of *Z. pseudotritici* (STIR04 2.2.1 (AFIQ01), STIR04 3.11.1 (AFIO01), STIR04 4.3.1 (AFIR01), STIR04 5.3 (AFIS01), STIR04 5.9.1 (AFIT01)) were obtained from NCBI under accession nos. PRJNA63035, PRJNA277173, PRJNA63037, PRJNA63039, PRJNA343335, PRJNA343334, PRJNA343333, PRJNA343332, PRJNA63049, PRJNA273516 and PRJNA46489. The genomic data of *Z. tritici* strain IPO87019 were obtained from JGI Genome Portal (Project ID: 1090932).

References

Ayliffe M, Sørensen CK. 2019. Plant nonhost resistance: paradigms and new environments. *Current Opinion in Plant Biology* 50: 104–113.

Bent AF, Mackey D. 2007. Elicitors, effectors, and *R* genes: the new paradigm and a lifetime supply of questions. *Annual Review of Phytopathology* 45: 399–436.

Bettgenhaeuser J, Gardiner M, Spanner R, Green P, Hernández-Pinzón I, Hubbard A, Ayliffe M, Moscou MJ. 2018. The genetic architecture of colonization resistance in *Brachypodium distachyon* to non-adapted stripe rust (*Puccinia striiformis*) isolates. *PLoS Genetics* 14: 1–26.

Bourras S, Kunz L, Xue M, Praz CR, Müller MC, Kälin C, Schläfli M, Ackermann P, Flückiger S, Parlange F et al. 2019. The *AvrPm3-Pm3* effector-NLR interactions control both race-specific resistance and host-specificity of cereal mildews on wheat. *Nature Communications* 10: 2292.

Brown JK, Chartrain L, Lasserre-Zuber P, Saintenac C. 2015. Genetics of resistance to *Zymoseptoria tritici* and applications to wheat breeding. *Fungal Genetics and Biology* 79: 33–41.

Brunner PC, McDonald BA. 2018. Evolutionary analyses of the avirulence effector AvrStb6 in global populations of *Zymoseptoria tritici* identify candidate amino acids involved in recognition. *Molecular Plant Pathology* 19: 1836–1846.

Buchan DWA, Jones DT. 2019. The PSIPRED protein analysis workbench: 20 years on. *Nucleic Acids Research* 47: W402–W407.

Chou S, Krasileva KV, Holton JM, Steinbrenner AD, Alber T, Staskawicz BJ. 2011. *Hyaloperonospora arabidopsidis* ATR1 effector is a repeat protein with distributed recognition surfaces. *Proceedings of the National Academy of Sciences, USA* 108: 13323–13328.

Cook DE, Mesarich CH, Thomma BPHJ. 2015. Understanding plant immunity as a surveillance system to detect invasion. *Annual Review of Phytopathology* 53: 541–563.

Cowger C, Brown JKM. 2019. Durability of quantitative resistance in crops: greater than we know? *Annual Review of Phytopathology* 57: 253–277.

De Jonge R, Van Esse HP, Maruthachalam K, Bolton MD, Santhanam P, Saber MK, Zhang Z, Usami T, Lievens B, Subbarao KV et al. 2012. Tomato immune receptor Ve1 recognizes effector of multiple fungal pathogens uncovered by genome and RNA sequencing. *Proceedings of the National Academy of Sciences, USA* 109: 5110–5115.

Dong S, Stam R, Cano LM, Song J, Sklenar J, Yoshida K, Bozkurt TO, Oliva R, Liu Z, Tian M et al. 2014. Effector specialization in a lineage of the Irish potato famine pathogen. *Science* 343: 552–555.

Dyrløv Bendtsen J, Nielsen H, von Heijne G, Brunak S. 2004. Improved prediction of signal peptides: SignalP 3.0. *Journal of Molecular Biology* 340: 783–795.

Feurtey A, Lorrain C, Croll D, Eschenbrenner C, Freitag M, Habig M, Haueisen J, Möller M, Schotanus K, Stukenbrock EH. 2019. Genome compartmentalization predates species divergence in the plant pathogen genus *Zymoseptoria*. *BMC Genomics* 21: 588.

Flor HH. 1971. Current status of the gene-for-gene concept. *Annual Review of Phytopathology* 9: 275–296.

Frantzeskakis L, Di Pietro A, Rep M, Schirawski J, Wu CH, Panstruga R. 2019. Rapid evolution in plant–microbe interactions – a molecular genomics perspective. *New Phytologist* 225: 1134–1142.

Fudal I, Ross S, Brun H, Besnard AL, Ermel M, Kuhn ML, Balesdent MH, Rouxel T. 2009. Repeat-induced point mutation (RIP) as an alternative mechanism of evolution toward virulence in *Leptosphaeria maculans*. *Molecular Plant–Microbe Interactions* 22: 932–941.

Gilbert B, Bettgenhaeuser J, Upadhyaya N, Soliveres M, Singh D, Park RF, Moscou MJ, Ayliffe M. 2018. Components of *Brachypodium distachyon* resistance to nonadapted wheat stripe rust pathogens are simply inherited. *PLoS Genetics* 14: 1–27.

Gilroy EM, Breen S, Whisson SC, Squires J, Hein I, Kaczmarek M, Turnbull D, Boevink PC, Lokossou A, Cano LM et al. 2011. Presence/absence, differential expression and sequence polymorphisms between *PiAVR2* and *PiAVR2*-like in *Phytophthora infestans* determine virulence on *R2* plants. *New Phytologist* 191: 763–776.

Goodwin SB, Ben M'Barek S, Dhillon B, Wittenberg AHJ, Crane CF, Hane JK, Foster AJ, Van der Lee TAJ, Grimwood J, Aerts A et al. 2011. Finished genome of the fungal wheat pathogen *Mycosphaerella graminicola* reveals dispensome structure, chromosome plasticity, and stealth pathogenesis. *PLoS Genetics* 7: e1002070.

Grandaubert J, Bhattacharyya A, Stukenbrock EH. 2015. RNA-seq-based gene annotation and comparative genomics of four fungal grass pathogens in the genus *Zymoseptoria* identify novel orphan genes and species-specific invasions of transposable elements. *G3: Genes, Genomes, Genetics* 5: 1323–1333.

Hartmann FE, Croll D. 2017. Distinct trajectories of massive recent gene gains and losses in populations of a microbial eukaryotic pathogen. *Molecular Biology and Evolution* 34: 2808–2822.

Hartmann FE, Sánchez-Vallet A, McDonald BA, Croll D. 2017. A fungal wheat pathogen evolved host specialization by extensive chromosomal rearrangements. *The ISME Journal* 11: 1189–1204.

Hogenhout SA, Van der Hoorn RAL, Terauchi R, Kamoun S. 2009. Emerging concepts in effector biology of plant-associated organisms. *Molecular Plant–Microbe Interactions* 22: 115–122.

Inoue Y, Vy TTP, Yoshida K, Asano H, Mitsuoka C, Asuke S, Anh VL, Cumagun CJR, Chuma I, Terauchi R *et al.* 2017. Evolution of the wheat blast fungus through functional losses in a host specificity determinant. *Science* 357: 80–83.

Jiquel A, Gervais J, Geistodt-Kiener A, Delourme R, Gay EJ, Ollivier B, Fudal I, Faure S, Balesdent MH, Rouxel T. 2021. A gene-for-gene interaction involving a 'late' effector contributes to quantitative resistance to the stem canker disease in *Brassica napus*. *New Phytologist* 231: 1510–1524.

Jones JDG, Dangl JL. 2006. The plant immune system. *Nature* 444: 323–329.

Jurrus E, Engel D, Star K, Monson K, Brandi J, Felberg LE, Brookes DH, Wilson L, Chen J, Liles K *et al.* 2018. Improvements to the APBS biomolecular solvation software suite. *Protein Science* 27: 112–128.

Kanzaki H, Yoshida K, Saitoh H, Fujisaki K, Hirabuchi A, Alaux L, Fournier E, Tharreau D, Terauchi R. 2012. Arms race co-evolution of *Magnaporthe oryzae* AVR-Pik and rice Pik genes driven by their physical interactions. *The Plant Journal* 72: 894–907.

Karasov TL, Shirsekar G, Schwab R, Weigel D. 2020. What natural variation can teach us about resistance durability. *Current Opinion in Plant Biology* 56: 89–98.

Kema G, Annone J, Sayoud R, Van Silfhout C, Van Ginkel M, De Bree J. 1996. Genetic variation for virulence and resistance in the wheat-*Mycosphaerella graminicola* pathosystem. 1. Interactions between pathogen isolates and host cultivars. *Phytopathology* 86: 200–212.

Kema GHJ, Gohari AM, Aouini L, Gibriel HAY, Ware SB, van Den Bosch F, Manning-Smith R, Alonso-Chavez V, Helps J, Barek SB *et al.* 2018. Stress and sexual reproduction affect the dynamics of the wheat pathogen effector AvrStb6 and strobilurin resistance. *Nature Genetics* 50: 375–380.

Kilaru S, Schuster M, Studholme D, Soanes D, Lin C, Talbot NJ, Steinberg G. 2015. A codon-optimized green fluorescent protein for live cell imaging in *Zymoseptoria tritici*. *Fungal Genetics and Biology* 79: 125–131.

Liao J, Huang H, Meusnier I, Adreit H, Ducasse A, Bonnot F, Pan L, He X, Kroj T, Fournier E *et al.* 2016. Pathogen effectors and plant immunity determine specialization of the blast fungus to rice subspecies. *eLife* 5: 1–18.

Lo Presti L, Lanver D, Schweizer G, Tanaka S, Liang L, Tollot M, Zuccaro A, Reissmann S, Kahmann R. 2015. Fungal effectors and plant susceptibility. *Annual Review of Plant Biology* 66: 513–545.

Lorrain C, Feurtey A, Ller MM, Haueisen J, Stukenbrock E. 2021. Dynamics of transposable elements in recently diverged fungal pathogens: lineage-specific transposable element content and efficiency of genome defenses. *G3: Genes, Genomes, Genetics* 11: jkab068.

Maqbool A, Saitoh H, Franceschetti M, Stevenson CEM, Uemura A, Kanzaki H, Kamoun S, Terauchi R, Banfield MJ. 2015. Structural basis of pathogen recognition by an integrated HMA domain in a plant NLR immune receptor. *eLife* 4: 213.

Marcel TC, Gorguet B, Ta MT, Kohutova Z, Vels A, Niks RE. 2008. Isolate specificity of quantitative trait loci for partial resistance of barley to *Puccinia hordei* confirmed in mapping populations and near-isogenic lines. *New Phytologist* 177: 743–755.

McDonald BA, Mundt CC. 2016. How knowledge of pathogen population biology informs management of Septoria tritici blotch. *Phytopathology* 106: 948–955.

McNally KE, Menardo F, Lüthi L, Praz CR, Müller MC, Kunz L, Ben-David R, Chandrasekhar K, Dinoor A, Cowger C *et al.* 2018. Distinct domains of the AVRPM3A2/F2 avirulence protein from wheat powdery mildew are involved in immune receptor recognition and putative effector function. *New Phytologist* 218: 681–695.

Meile L, Croll D, Brunner PC, Plissonneau C, Hartmann FE, McDonald BA, Sánchez-Vallet A. 2018. A fungal avirulence factor encoded in a highly plastic genomic region triggers partial resistance to Septoria tritici blotch. *New Phytologist* 219: 1048–1061.

Motteram J, Lovegrove A, Pirie E, Marsh J, Devonshire J, van de Meene A, Hammond-Kosack K, Rudd JJ. 2011. Aberrant protein N-glycosylation impacts upon infection-related growth transitions of the haploid plant-pathogenic fungus *Mycosphaerella graminicola*. *Molecular Microbiology* 81: 415–433.

Niks RE, Qi X, Marcel TC. 2015. Quantitative resistance to biotrophic filamentous plant pathogens: concepts, misconceptions, and mechanisms. *Annual Review of Phytopathology* 53: 445–470.

Panstruga R, Moscou MJ. 2020. What is the molecular basis of nonhost resistance? *Molecular Plant–Microbe Interactions* 33: 1253–1264.

Plissonneau C, Hartmann FE, Croll D. 2018. Pangenome analyses of the wheat pathogen *Zymoseptoria tritici* reveal the structural basis of a highly plastic eukaryotic genome. *BMC Biology* 16: 5.

Plissonneau C, Stürchler A, Croll D. 2016. The evolution of orphan regions in genomes of a fungal pathogen of wheat. *mBio* 7: e01231-16.

Poland JA, Balint-Kurti PJ, Wisser RJ, Pratt RC, Nelson RJ. 2009. Shades of gray: the world of quantitative disease resistance. *Trends in Plant Science* 14: 21–29.

Poppe S, Dorsheimer L, Happel P, Stukenbrock EH. 2015. Rapidly evolving genes are key players in host specialization and virulence of the fungal wheat pathogen *Zymoseptoria tritici* (*Mycosphaerella graminicola*). *PLoS Pathogens* 11: e1005055.

Qutob D, Patrick Chapman B, Gijzen M. 2013. Transgenerational gene silencing causes gain of virulence in a plant pathogen. *Nature Communications* 4: 1349.

Ravensdale M, Bernoux M, Ve T, Kobe B, Thrall PH, Ellis JG, Dodds PN. 2012. Intramolecular interaction influences binding of the flax L5 and L6 resistance proteins to their AvrL567 ligands. *PLoS Pathogens* 8: e1003004.

Rouxel T, Penaud A, Pinochet X, Brun H, Gout L, Delourme R, Schmit J, Balesdent MH. 2003. A 10-year survey of populations of *Leptosphaeria maculans* in France indicates a rapid adaptation towards the *Rlm1* resistance gene of oilseed rape. *European Journal of Plant Pathology* 109: 871–881.

RStudio Team. 2015. RSTUDIO: integrated development for R. Boston, MA, USA: RStudio.

Ruijter JM, Ramakers C, Hoogaars WMH, Karlen Y, Bakker O, van den Hoff MJB, Moorman AFM. 2009. Amplification efficiency: linking baseline and bias in the analysis of quantitative PCR data. *Nucleic Acids Research* 37: e45.

Sánchez-Martín J, Keller B. 2021. NLR immune receptors and diverse types of non-NLR proteins control race-specific resistance in *Triticeae*. *Current Opinion in Plant Biology* 62: 102053.

Sánchez-Vallet A, Fouché S, Fudal I, Hartmann FE, Soyer JL, Tellier A, Croll D. 2018. The genome biology of effector gene evolution in filamentous plant pathogens. *Annual Review of Phytopathology* 56: 21–40.

Schneider CA, Rasband WS, Eliceiri KW. 2012. NIH IMAGE to IMAGEJ: 25 years of image analysis. *Nature Methods* 9: 671–675.

Schrodinger LLC. 2015. *The PYMOL molecular graphics system, v.1.8.* New York, NY, USA: Schrodinger.

Schulze-Lefert P, Panstruga R. 2011. A molecular evolutionary concept connecting nonhost resistance, pathogen host range, and pathogen speciation. *Trends in Plant Science* 16: 117–125.

Sperschneider J, Gardiner DM, Dodds PN, Tini F, Covarelli L, Singh KB, Manners JM, Taylor JM. 2016. EFFECTORP: predicting fungal effector proteins from secretomes using machine learning. *New Phytologist* 210: 743–761.

Stephens C, Ölmez F, Blyth H, McDonald M, Bansal A, Turgay EB, Hahn F, Saintenac C, Nekrasov V, Solomon P *et al.* 2021. Remarkable recent changes in the genetic diversity of the avirulence gene AvrStb6 in global populations of the wheat pathogen *Zymoseptoria tritici*. *Molecular Plant Pathology* 22: 1121–1133.

Stergiopoulos I, de Wit PJGM. 2009. Fungal effector proteins. *Annual Review of Phytopathology* 47: 233–263.

Stewart EL, Hagerty CH, Mikaberidze A, Mundt CC, Zhong Z, McDonald BA. 2016. An improved method for measuring quantitative resistance to the wheat pathogen *Zymoseptoria tritici* using high-throughput automated image analysis. *Phytopathology* 106: 782–788.

Stukenbrock EH, Banke S, Javan-Nikkhah M, McDonald BA. 2007. Origin and domestication of the fungal wheat pathogen *Mycosphaerella graminicola* via sympatric speciation. *Molecular Biology and Evolution* 24: 398–411.

Stukenbrock EH, Bataillon T, Dutheil JY, Hansen TT, Li R, Zala M, McDonald BA, Wang J, Schierup MH. 2011. The making of a new pathogen: insights from comparative population genomics of the domesticated wheat pathogen *Mycosphaerella graminicola* and its wild sister species. *Genome Research* 21: 2157–2166.

Stukenbrock EH, Quaedvlieg W, Javan-Nikhah M, Zala M, Crous PW, McDonald BA. 2012. *Zymoseptoria ardabiliae* and *Z. pseudotritici*, two

progenitor species of the septoria tritici leaf blotch fungus *Z. tritici* (synonym: *Mycosphaerella graminicola*). *Mycologia* **104**: 1397–1407.

Torriani SFF, Stukenbrock EH, Brunner PC, McDonald BA, Croll D. 2011. Evidence for extensive recent intron transposition in closely related fungi. *Current Biology* **21**: 2017–2022.

Toruño TY, Stergiopoulos I, Coaker G. 2016. Plant-pathogen effectors: cellular probes interfering with plant defenses in spatial and temporal manners. *Annual Review of Phytopathology* **54**: 419–441.

Walton JD. 1996. Host-selective toxins: agents of compatibility. *Plant Cell* **8**: 1723–1733.

Wang CIA, Gunčar G, Forwood JK, Teh T, Catanzariti AM, Lawrence GJ, Loughlin FE, Mackay JP, Schirra HJ, Anderson PA *et al.* 2007. Crystal structures of flax rust avirulence proteins AvrL567-A and -D reveal details of the structural basis for flax disease resistance specificity. *Plant Cell* **19**: 2898–2912.

Wu J, Kou Y, Bao J, Li Y, Tang M, Zhu X, Ponaya A, Xiao G, Li J, Li C *et al.* 2015. Comparative genomics identifies the *Magnaporthe oryzae* avirulence effector *AvrPi9* that triggers *Pi9*-mediated blast resistance in rice. *New Phytologist* **206**: 1463–1475.

Yang J, Anishchenko I, Park H, Peng Z, Ovchinnikov S, Baker D. 2020. Improved protein structure prediction using predicted interresidue orientations. *Proceedings of the National Academy of Sciences, USA* **117**: 1496–1503.

Ye Y, Godzik A. 2003. Flexible structure alignment by chaining aligned fragment pairs allowing twists. *Bioinformatics* **19**: 246–255.

Yechilevich-Auster M, Levi E, Eyal Z. 1983. Assessment of interactions between cultivated and wild wheats and *Septoria tritici*. *Phytopathology* **73**: 1077.

Zenbayashi-Sawata K, Ashizawa T, Koizumi S. 2005. *Pi34-AVRPi34*: a new gene-for-gene interaction for partial resistance in rice to blast caused by *Magnaporthe grisea*. *Journal of General Plant Pathology* **71**: 395–401.

Zhan J, Linde CC, Jurgens T, Merz U, Steinebrunner F, McDonald BA. 2005. Variation for neutral markers is correlated with variation for quantitative traits in the plant pathogenic fungus *Mycosphaerella graminicola*. *Molecular Ecology* **14**: 2683–2693.

Zhang X, Farah N, Rolston L, Ericsson DJ, Catanzariti AM, Bernoux M, Ve T, Bendak K, Chen C, Mackay JP *et al.* 2018. Crystal structure of the *Melampsora lini* effector AvrP reveals insights into a possible nuclear function and recognition by the flax disease resistance protein P. *Molecular Plant Pathology* **19**: 1196–1209.

Zhong Z, Marcel TC, Hartmann FE, Ma X, Plissonneau C, Zala M, Ducasse A, Confais J, Compain J, Lapalu N *et al.* 2017. A small secreted protein in *Zymoseptoria tritici* is responsible for avirulence on wheat cultivars carrying the *Stb6* resistance gene. *New Phytologist* **214**: 619–631.

Zwiers L-H, De Waard MA. 2001. Efficient *Agrobacterium tumefaciens*-mediated gene disruption in the phytopathogen *Mycosphaerella graminicola*. *Current Genetics* **39**: 388–393.

Supporting Information

Additional Supporting Information may be found online in the Supporting Information section at the end of the article.

Fig. S1 DNA sequence alignment of homologues of *Avr3D1* identified in different *Zymoseptoria* species.

Fig. S2 Cloning strategy for swapping the coding DNA sequence of *Avr3D1* for ectopic expression.

Fig. S3 Independent transformants of the Avr3D1 isogenic lines expressing different *Avr3D1* alleles.

Fig. S4 Different Avr3D1 isoforms lead to different magnitudes of pathogen infection.

Fig. S5 Isoforms of Avr3D1 from AUS1B1 and AUS1E5 are not recognized by the resistant cultivar Runal.

Fig. S6 Different isoforms of Avr3D1 lead to different magnitudes of pathogen infection in different wheat lines.

Fig. S7 Maximum likelihood tree of 33 Avr3D1 isoforms identified in 135 *Zymoseptoria tritici* strains.

Fig. S8 3D structure model comparison of Avr3D1 isoforms in 3D1 and 3D7 strains.

Fig. S9 Protein sequence comparison between Avr3D1 and its homologues in different *Zymoseptoria* species.

Fig. S10 Homologues of Avr3D1 present in different *Zymoseptoria* species trigger defenses in wheat.

Table S1 Primers used in this study.

Table S2 Number of replicates in each infection assay.

Table S3 Raw data of infection assays.

Table S4 Raw data of Fig. 1.

Video S1 Confocal laser scanning microscopy video of GFP-tagged *Zymoseptoria tritici* mutant without Avr3D1 (*Δavr3D1*) while in contact with wheat stomata.

Video S2 Confocal laser scanning microscopy video of GFP-tagged *Zymoseptoria tritici* mutant expressing *Avr3D1$_{3D1}$* while in contact with wheat stomata.

Video S3 Confocal laser scanning microscopy video of GFP-tagged *Zymoseptoria tritici* mutant expressing *Avr3D1$_{ISR398}$* transformant 1 while in contact with wheat stomata.

Video S4 Confocal laser scanning microscopy video of GFP-tagged *Zymoseptoria tritici* mutant expressing *Avr3D1$_{ISR398}$* transformant 2 while in contact with wheat stomata.

Please note: Wiley is not responsible for the content or functionality of any Supporting Information supplied by the authors. Any queries (other than missing material) should be directed to the *New Phytologist* Central Office.